The photoionisation of two phenylcarbenes and their diazirine precursors investigated using synchrotron radiation

Bastian Noller,[a] Patrick Hemberger,[a] Ingo Fischer,*[a] Christian Alcaraz,*[b] Gustavo A. Garcia*[c] and Héloïse Soldi-Lose[c]

Received 6th January 2009, Accepted 20th March 2009
First published as an Advance Article on the web 22nd April 2009
DOI: 10.1039/b823269e

Two phenylcarbenes, chlorophenylcarbene (CPC) and trifluoromethylphenylcarbene (TFPC), were generated by jet flash pyrolysis of diazirine precursors. Their photoionisation was studied by photoelectron–photoion coincidence spectroscopy using synchrotron radiation. For CPC we determined an adiabatic ionisation energy (IE) of 8.15 eV and a vertical IE of 9.3 eV. For TFPC we obtained an adiabatic IE of 8.47 eV and a vertical IE of 8.95 eV. The photoelectron spectra are broad and unstructured due to a large increase in the angle between the phenyl group, carbene centre and the substituent (Cl or CF_3). The geometry change upon ionisation is more pronounced for CPC. Being a singlet arylcarbene, CPC is more strongly bent in the neutral ground state than the triplet TFPC. In addition, the bond between the carbenic centre and the chlorine atom shortens upon ionisation, because the radical cation is stabilised by the non-bonding electrons of the Cl through a mesomeric effect. The photoionisation and dissociative photoionisation of the diazirine precursors are also explored. The CPC precursor, 3-chloro-3-phenyldiazirine, undergoes complete dissociative photoionisation and only the CPC^+ fragment is observed above 8.8 eV. For 3-trifluoromethyl-3-phenyldiazirine some molecular ions can be observed above 9.05 eV. However, dissociative photoionisation also sets in right at the ionisation threshold. A fit to the data yields an appearance energy of AE (0 K) $\approx$ 9.27 eV.

Introduction

In this paper we present a study on the photoionisation of two phenylcarbenes, chlorophenylcarbene (CPC) and trifluoromethylphenylcarbene (TFPC), and on the dissociative photoionisation of their corresponding diazirine precursors, CP-N_2 and TFP-N_2.

Ionisation and appearance energies (IE and AE) are important gas phase thermochemical properties since they permit the derivation of other quantities, such as binding energies or heats of formation.[1,2] However, for reactive intermediates such as radicals and carbenes, they are difficult to obtain because a clean generation of the intermediates at a number density sufficient for photoionisation experiments is challenging. Although accurate IE values have been computed for some small radicals at a high level of theory,[3] calculations with chemical accuracy are computationally expensive and inadequate for larger molecules. In previous studies we have shown that an excellent experimental approach is the generation of reactive intermediates by flash pyrolysis with subsequent ionisation by synchrotron radiation (SR). Synchrotron beamlines provide short-wavelength radiation tunable over a large energy range and are thus well suited for experiments on species with unknown ionisation properties. For instance, the thresholds for the dissociative ionisation of allyl, ethyl and propargyl species have been identified in earlier experiments.[4–6] Here, this work is extended to two phenylcarbenes. Carbenes with their large number of low-lying electronic states constitute model systems for non-adiabatic interactions and serve as benchmarks for computational methods.[7] Therefore we recently studied several phenylcarbenes by femtosecond time-resolved photoelectron spectroscopy and obtained detailed insight into their excited state dynamics.[8] It showed, however, that the information available from the femtosecond spectra was limited by the lack of data on the ionic ground state. We therefore measured adiabatic and vertical ionisation energies for chlorophenylcarbene (CPC) and trifluoromethylphenylcarbene (TFPC), both species depicted in Scheme 1, by photoelectron and photoion imaging using SR as the photon source. In particular CPC serves as a model for carbene chemistry in general. A reasonable amount of experimental data exists for the neutral ground state as well as the kinetics

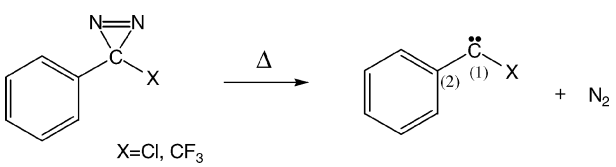

Scheme 1 Both phenylcarbenes are generated by jet flash pyrolysis of diazirines.

[a] *Institute of Physical Chemistry, University of Würzburg, Am Hubland, D-97074, Würzburg, Germany. E-mail: ingo@phys-chemieuni-wuerzburg.de*
[b] *Laboratoire de Chimie-Physique, UMR 8000 CNRS & Université Paris-Sud 11, F-91405, Orsay Cedex, France. E-mail: christian.alcaraz@lcp.u-psud.fr*
[c] *Synchrotron SOLEIL, L'Orme des Merisiers, Saint Aubin-BP 48, F-91192, Gif-sur-Yvette, France. E-mail: gustavo.garcia@synchrotron-soleil.fr*

of several condensed-phase reactions.[9–11] The electronic structure of the neutral ground state has been computed by *ab initio* methods.[12] While chlorophenylcarbene has a singlet ground state,[12] trifluoromethylphenylcarbene has a triplet ground state, as shown by ESR-experiments[13] and confirmed by computations performed by our group.[14]

In the case of diazirines, additional interest arises from their application in photoaffinity labelling, where photochemical activation induces the loss of nitrogen from functionalised diazirine precursors generating carbenes, which then form covalent bonds with specific target receptors.[15] The properties of diazirines are thus of considerable interest in their own right.

Experimental

Experiments were carried out at the DESIRS beamline of the SOLEIL storage ring in St. Aubin (France), which was partially transferred from the SU5 beamline at Super ACO.[16] The storage ring was operating in multi-bunch mode with 3/4 filling. The electromagnetic undulator OPHELIE2 provides tunable radiation in the energy range between 5 and 40 eV.[17] The wavelength is selected by a normal incidence monochromator with a focal length of 6.65 m.[16] The newly added monochromator grating (200 gr mm^{-1}) was employed, which provides a high photon flux with a photon resolution of 5 meV at 9 eV photon energy with a 100 μm exit slit. In the scanned energy range (7–10 eV) a photon flux of more than 10^{12} photons s^{-1} was available. The higher harmonics originating from the undulator were eliminated by a gas filter filled with Ar.[18] The pressure of argon in the gas filter was set to 0.23 mbar, which corresponds to an attenuation factor of around 100.

Experiments were performed in the differentially pumped vacuum chamber SAPHIRS[19] and various techniques were used to study the photoionisation of carbenes cooled in a free jet. In particular the (threshold) photoelectron–photoion coincidence ((T)PEPICO) technique was applied.[20,21]

The SAPHIRS chamber is equipped with a velocity map imaging (VMI)[22] device coupled to a Wiley–McLarenTOF spectrometer (DELICIOUS II).[23] Briefly, electrons and ions were extracted from the interaction region by static fields of either 95 or 190 V cm^{-1} and detected on an imaging detector equipped with a delay line anode.[24] Ions were further accelerated with static fields of 333 or 666 V cm^{-1} which were chosen to achieve time focusing according to the Wiley–McLaren conditions. Detection of an electron opens a time gate for ion detection, permitting to register them in coincidence with electrons.

TPEPICO spectra were obtained by scanning the photon energy over the ionisation threshold in either 10 or 4 meV steps, while recording the ion signals in coincidence with threshold electrons, which were selected with an energy resolution of 3–10 meV. The resulting spectra were normalised by the photon flux given by a calibrated gold grid situated before the experimental chamber.

In addition to the TPEPICO measurements, photoelectron images were recorded at fixed photon energies. The subsequent treatment of these images with the pBasex algorithm[25] yielded the conventional photoelectron spectra (PES).

A continuous molecular beam was used in all the experiments. The design of the pyrolysis source is described elsewhere.[26] A heated SiC tube was mounted onto a faceplate of a General Valve, employing a faceplate with a 0.1 mm orifice, operated without poppet and augmented by a water cooling system. Two electrodes were fixed as near as possible at the end of the SiC tube to minimise bimolecular reactions. 3-Trifluoromethyl-3-phenyldiazirine (TFP-diazirine, TFP-N_2) and 3-chloro-3-phenyldiazirine (CP-diazirine, CP-N_2) were used as precursors. It is known that diazirines are ideally suited to generate carbenes.[27] The compounds were synthesised following literature procedures.[28,29] Both precursors were seeded in 0.5 bar (absolute) of Ar and expanded through the SiC tube. The heating power was adjusted for optimal precursor conversion. In all experiments the SiC tube was only weakly heated (faint red glow), and low temperatures proved to be sufficient for complete conversion of the precursor. The quality of the molecular beam was optimised and verified by ion velocity map imaging, where the image shows the amount of supersonic fast ions with respect to the thermal background. The ratio of supersonic to thermal was maximised by the distance and alignment of the nozzle with respect to the skimmer.

Results and discussion

(a) Mass spectra

In experiments on reactive intermediates it has to be checked whether the species of interest is formed cleanly. Therefore mass spectra of the precursors have been recorded at photon energies above the ionisation threshold of the carbenes. Fig. 1 shows mass spectra of TFP-diazirine, recorded at a photon

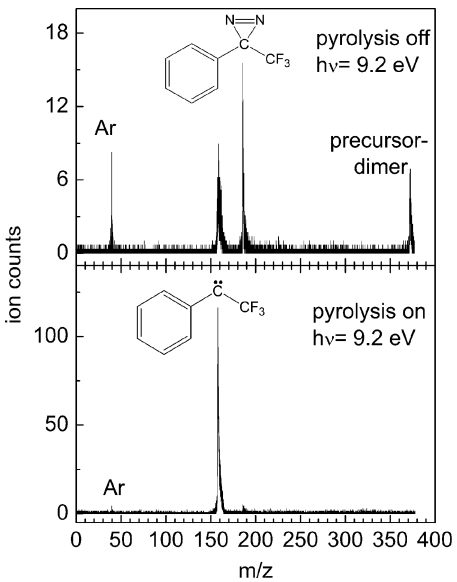

Fig. 1 Mass spectra of $TFPC^+$ with pyrolysis off (upper trace) and on (lower trace), corresponding to 100 s averaging. The lower graph shows that almost quantitative conversion of the precursor is achieved and no side products are visible.

energy of 9.2 eV. Without pyrolysis (upper trace) the spectrum is dominated by the diazirine precursor (m/z = 186). Some dissociative photoionisation occurs, as shown by the signal at m/z = 158 which corresponds to the carbene fragment $TFPC^+$. In addition, a signal appears at m/z = 372 which is attributed to a weakly bound diazirine dimer. This indicates that the temperature in the beam is sufficiently low to permit cluster formation. The argon signal was due to the presence of some second harmonic radiation that was not absorbed by the gas filter and served as a mass reference. When the pyrolysis is turned on (lower trace), the carbene signal increases significantly and dominates the mass spectrum. Note the different y-scale in the two traces of Fig. 1. Almost quantitative conversion of the diazirine precursor is achieved and no side products are visible. The relative increase in the ion signal indicates either a large ionisation cross section of the carbene or a large contribution of neutral dissociation in the diazirine, which competes with ionisation. In Fig. 2 the mass spectra of CPC are depicted. Due to a shorter accumulation time the signal-to-noise ratio is significantly lower than in the case of TFPC. In the mass spectrum without pyrolysis (upper trace) a carbene signal is visible, but no precursor signal. This indicates complete dissociative photoionisation at this wavelength. When the pyrolysis is turned on, an additional signal at mass m/z = 41 appears, which is attributed to allyl, $C_3H_5^+$, and is due to the pyrolysis of residual C_3H_5I which was used in calibration experiments. A small signal also appears at m/z = 89 and corresponds to $C_7H_5^+$ (Cl-loss from carbene). It is presumably a side product from the pyrolysis and does not originate from dissociative photoionisation of the precursor. The signal was too small to be analysed any further.

At first glance it is not evident whether the CPC^+ with pyrolysis turned on does indeed originate from pyrolysis of the diazirine. However, recording ion images did aid in the optimisation of carbene generation. Fig. 3 shows an ion image with pyrolysis on, recorded at 9 eV. The CPC^+ has a narrow kinetic energy distribution which is comparable to that of the

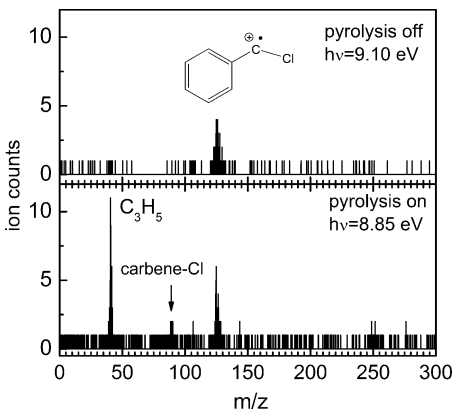

Fig. 2 Mass spectra of CPC^+ with pyrolysis off (upper trace) and on (lower trace). Both spectra were averaged for 25 s. Again almost quantitative conversion of the precursor is achieved and no side products are visible. No signal from the diazirine precursor is discernible, indicating complete dissociative photoionisation. The signal at m/z = 41 originates from earlier calibration experiments with C_3H_5I.

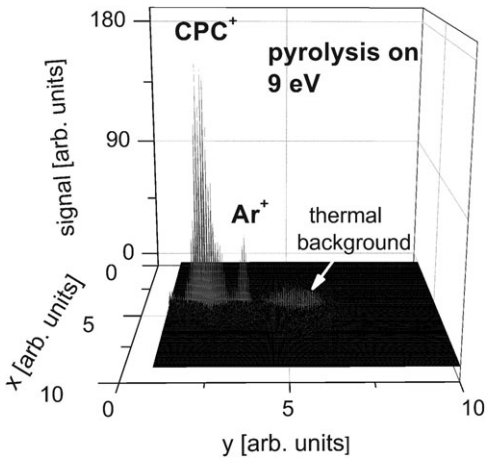

Fig. 3 Ion image of CPC with the pyrolysis on recorded at 9 eV. The narrow kinetic energy distribution indicates that carbene originates from pyrolysis and not from dissociative photoionisation. This way complete conversion of the precursor in the pyrolysis could be ensured.

Ar along the direction perpendicular to the molecular beam. Thus we conclude that no CPC^+ fragments coming from dissociative ionisation are evident at 9.0 eV, since they would appear in the ion imaging as outer, concentric rings around the parent. Similar observations were made for TFP-N_2. Therefore we were able to ensure complete conversion of the precursor in all experiments by monitoring the ion images. This has been discussed in detail elsewhere.[14]

(b) Dissociative photoionisation of diazirines

In order to understand the ionisation of reactive intermediates, the dissociative ionisation of the precursor has to be investigated first, because this process may provide an additional source of the reactive species. In experiments on TFP-diazirine without pyrolysis we monitored the ion signal of all masses present in the mass spectrum of Fig. 1 (upper trace) as a function of photon energy. The resulting data are shown in Fig. 4. At each photon energy data were averaged for 7s. The signals of both the diazirine precursor and the carbene increase

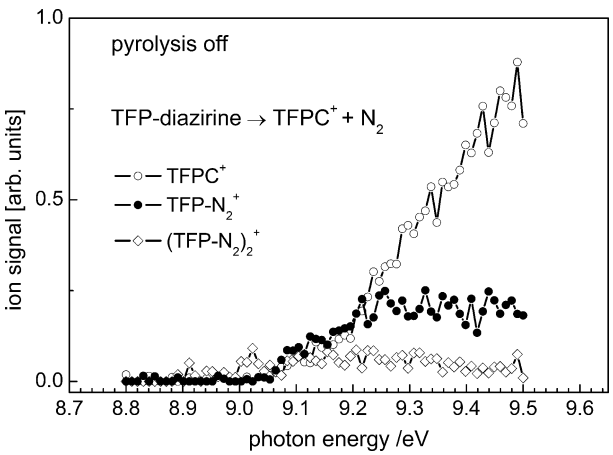

Fig. 4 Ion yield curves of the masses appearing in the photoionisation of the TFP- N_2, pyrolysis off. Dissociative photoionisation at the ionisation threshold around 9.05 eV is evident.

above 9.05 eV. Part of the diazirine had dissociated already at the ionisation threshold according to the reaction

$$\text{TFP-N}_2 + h\nu \rightarrow \text{TFPC}^+ + \text{N}_2 + e^- \qquad (1)$$

The ionisation of the precursor dimer sets in slightly earlier, at around 8.9 eV, and stays at a low level up to 9.5 eV.

More energetically accurate data can be obtained when only ions detected in coincidence with threshold or near-threshold electrons (TPEPICO) are recorded. In this way, the internal energy deposited onto the parent ion is precisely known. For further data analysis we selected only ions that were associated with threshold electrons, detected with a kinetic energy resolution of 10 meV. Fig. 5 shows a breakdown diagram of the TFP-N_2 parent ion and the TFPC fragment ion. Due to noise in the data a five-point average is plotted in the figure and the fractional abundance in the low and high photon energy limits deviates from 0 or 100%, respectively. It can be observed that the signal rise is much steeper and does not increase any further beyond 9.3 eV. The detailed analysis of such breakdown diagrams is described in the literature.[30–32] Since in our experiments the noise level is high and the temperature in the beam is not well known, we employed a simplified approach: we fitted the decay of the parent ion signal and the baseline signal at high photon energies by a straight line and assumed that the crossing point of the two lines around 9.30 eV constitutes the 0 K appearance energy. However, the smoothing of the data will modify the steepness of the step and move the crossing point to higher energies. The influence of this term can be calculated by multiplying the scan step size (10 meV) by 2.5 due to the five-point average, leading to a 25 meV shift. In addition, the 10 meV electron energy resolution has to be taken into account. We therefore arrive at an approximated appearance energy of AE (0 K) $\approx$ 9.27 eV.

The ion yield of the CPC^+ fragment from CP-N_2, detected in coincidence with threshold electrons, is depicted in Fig. 6. No signal from the precursor was observed, indicating a complete dissociative ionisation of the diazirine according to:

$$\text{CP-N}_2 + h\nu \rightarrow \text{CPC}^+ + \text{N}_2 + e^- \qquad (2)$$

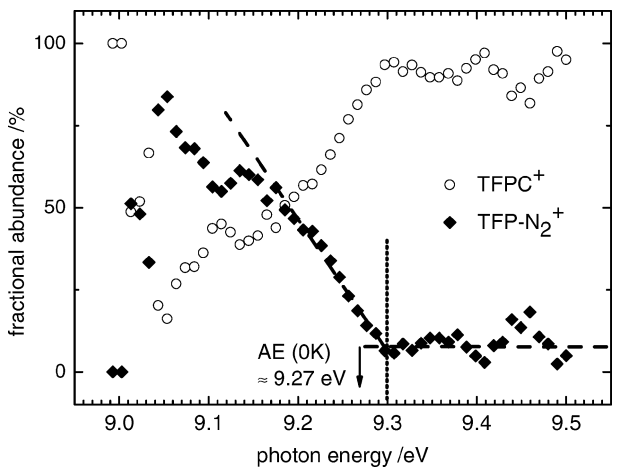

Fig. 5 Breakdown diagram of the TFP-N_2^+/$TFPC^+$ ions detected in coincidence with threshold electrons. Data analysis yields an approximate appearance energy $AE_{0K} \approx 9.27$ eV.

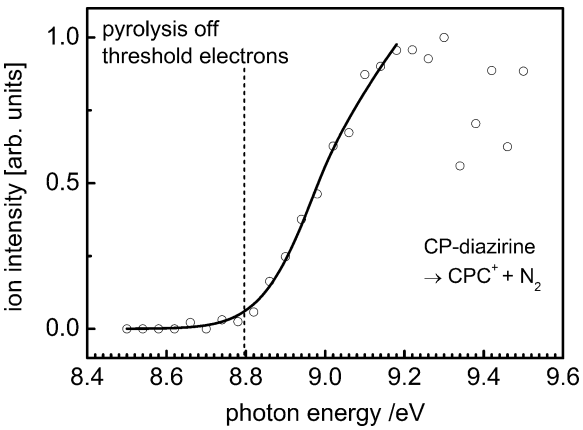

Fig. 6 The signal of CPC^+ fragment ions detected in coincidence with threshold electrons appearing in the photoionisation of CP-diazirine, pyrolysis off. The precursor undergoes complete dissociative ionisation. The process sets in above 8.8 eV.

Dissociative photoionisation sets in above 8.8 eV. Since the onset is probably determined by Franck–Condon factors, no meaningful appearance energy can be extracted. Note that it is not possible with our apparatus to extract a kinetic energy release from the time-of-flight peak widths that would help us to extract a meaningful AE (0 K).

(c) Computations

To aid in the interpretation of the experiment, we carried out hybrid density functional theory (DFT) computations. We employed the B3LYP correlation functional[33] with a 6-311^{++}G** basis set as implemented in the Gaussian 03 program package[34] and used the tight convergence criteria with an ultrafine grid. The geometry optimisation used the modified GDIIS algorithm.[35] This method is known to give good results for calculations on phenylcarbenes[12] and showed negligible spin contaminations in our computations. For both carbenes the geometry of the neutral and the ionic ground states was computed.[36] While C_s symmetry was found in both neutral and cationic ground states of CPC, TFPC has no symmetry due to a slight torsion of the CF_3 group out of the mirror plane. However, the torsional barrier of the CF_3 group is low, thus we expect an effective C_s symmetry as well. In CPC the highest occupied molecular orbital (HOMO) can be described as an sp^2-orbital at the carbene centre.[12] In the triplet ground state of TFPC one electron is promoted to the $C_{(1)}$ p-orbital, which interacts with the aromatic π-system. Upon ionisation, the electron is removed from the latter orbital. The geometric parameters that show the biggest change in the ionisation process are summarised in Table 1.

Table 1 The most important geometry parameters and vibrational wavenumbers for the neutral and cationic ground states of the two carbenes, calculated at B3LYP/6-311^{++}G** level of theory

	CPC	CPC^+	TFPC	$TFPC^+$
$R(C_{(1)}–C_{(2)})$/Å	1.45	1.37	1.39	1.35
$R(C_{(1)}–X)$/Å	1.75	1.62	1.46	1.50
θ ($C_{(1)}–C_{(2)}–X$)	112.5°	137.3°	137.5°	142.5°
$\nu(C_{(1)}–C_{(2)}–X$ bent)/cm^{-1}	200	145	89	114

These are the bond length between the carbene centre $C_{(1)}$ and the neighbouring carbon atom in the phenyl ring $C_{(2)}$, $R(C_{(1)}–C_{(2)})$, see Scheme 1 for the labelling of the atoms, the bond length between $C_{(1)}$ and the substituent X (which is either Cl or the carbon of the CF_3 group), $R(C_{(1)}–X)$, and the angle θ between $C_{(1)}$, $C_{(2)}$ and X, $\theta(C_{(1)}–C_{(2)}–X)$. Changes in the phenyl group are of minor importance in the photoionisation process. In CPC, upon removal of an electron, the angle θ increases significantly from 112.5° to 137.3°. In TFPC, on the other hand, θ increases only from 137.5° to 142.1°. In addition one finds changes in the bond length upon ionisation. There is a pronounced reduction in both bond lengths in CPC. In TFPC, on the other hand, the bond length between $C_{(1)}$ and the CF_3 group increases slightly, while $R(C_{(1)}–C_{(2)})$ also decreases. Based on the calculations, we expect the $C_{(1)}–C_{(2)}–X$ bending vibration to be the most important low-wavenumber vibration in both species. In the cation, wavenumbers of 114 and 145 cm^{-1} were computed for this mode in TFPC and CPC, respectively. There are other low-wavenumber vibrations in both carbenes and cations, but most of them cannot be assigned to a simple bond change.

Since the cations of both carbenes are open-shell systems, low-lying excited electronic states can be expected. In fact, a number of electronically excited states were computed by time-dependent density functional theory (TD-DFT) to lie between roughly 2 and 3 eV above the ionic ground state in both carbenes. However, none of them is low enough in energy to play a role in the energy region investigated here. The adiabatic ionisation energies were obtained from the difference between the zero point energies of the fully optimised structure of the neutral carbene and its cation. The vertical IE values were calculated using the neutral ground state equilibrium structure for both species. The computed adiabatic and vertical ionisation energies are 7.41 eV and 8.20 eV for CPC, and 7.93 eV and 8.15 eV for TFPC. All experimental and computational values are summarised in Table 2.

We also computed the geometry of the neutral and ionic ground states of both diazirine precursors. We identified energy minima on the ionic ground state surface of both diazirines, although the dissociation to a carbene cation plus N_2 was computed to be exothermic (79 and 136 kJ mol^{-1} for TFP^+-N_2 and CP^+-N_2, respectively). The HOMO of both extends over the whole molecule, including the N═N double bond as well as the phenyl ring. In CP-diazirine the distance between $C_{(1)}$ and the N═N moiety increases upon ionisation from 1.46 Å to 1.57 Å. In addition, $R(C_{(1)}–C_{(2)})$, $R(C_{(1)}–X)$ and R(N═N) shorten significantly (*cf.* Table 1), indicating a tendency to ring cleavage and liberation of the N_2-group. In TFP-diazirine the same tendencies are observed, as summarised in Table 3. However, the $C_{(1)}–CF_3$ bond length increases slightly upon ionisation, whereas in CP-diazirine a significant decrease in the $C_{(1)}$–Cl bond length is calculated.

Table 2 Summary of ionisation energies for chlorophenylcarbene (CPC) and trifluoromethylphenylcarbene (TFPC). All values are given in eV

	IE_{ad} (exp.)	IE_{vert} (exp.)	IE_{ad} (comp.)	IE_{vert} (comp.)
CPC	8.15	9.30	7.41	8.20
TFPC	8.47	8.95	7.93	8.15

Table 3 The most important geometry parameters for the diazirine-precursors and their corresponding cations, calculated at B3LYP/6-311^{++}G** level of theory

	CP–N_2	$(CP–N_2)^+$	TFP–N_2	$(TFP–N_2)^+$
$R(C_{(1)}–N_2)$/Å	1.46	1.57	1.48	1.56
$R(C_{(1)}–C_{(2)})$/Å	1.49	1.43	1.49	1.43
$R(C_{(1)}–X)$/Å	1.77	1.71	1.51	1.53
R(N═N)	1.23	1.18	1.22	1.18

(d) Ionisation energies of carbenes

A major goal of the measurements was to determine the vertical and adiabatic ionisation energies of both carbenes. Therefore a velocity-mapped photoelectron image of TFPC was recorded at a photon energy of 9.3 eV, and data were accumulated for 1345 s. Only electrons that arrived in coincidence with a TFPC cation were considered in the data analysis. Since no anisotropies were visible in the data, the image was averaged over all angles and converted through Abel inversion to a conventional photoelectron spectrum, depicted in Fig. 7. It consists of a broad and unstructured band, indicating a considerable geometry change upon ionisation. The signal starts to rise at around 0.9 eV from which an adiabatic IE of 8.4 eV could be derived. From the band maximum at 0.35 eV we derive a vertical ionisation energy: $IE_{vert} = 8.95 \pm 0.05$ eV.

Adiabatic ionisation energies can in principle be obtained from a Franck–Condon (FC) simulation[37] to the photoelectron spectrum. We carried out such a FC-simulation using the minimum energy geometries for neutral and cationic ground states obtained from the *ab initio* computations. Due to the size of the molecule only a region of 0.5 eV was simulated and the number of simultaneously excited modes had to be restricted to 7. The resulting stick spectrum is given for comparison in Fig. 7. It is based on an adiabatic IE of 8.4 eV. As visible it fits the experimental spectrum only

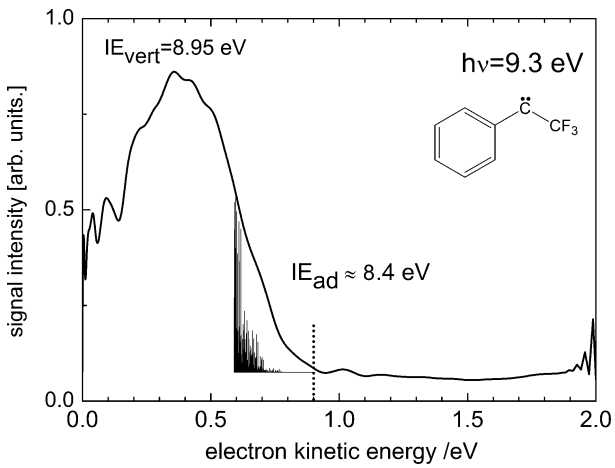

Fig. 7 From the photoelectron spectrum of TFPC we extract a vertical ionisation energy of 8.95 eV. A Franck–Condon simulation, based on the computed geometry and an $IE_{ad} = 8.4$ eV, is depicted for comparison.

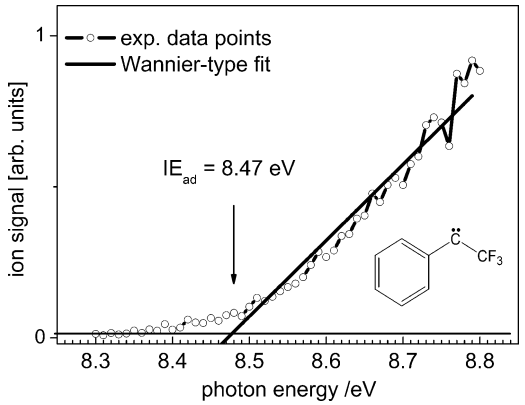

Fig. 8 From the photoionisation efficiency curve of $TFPC^+$ an IE_{ad} = 8.47 eV can be extracted.

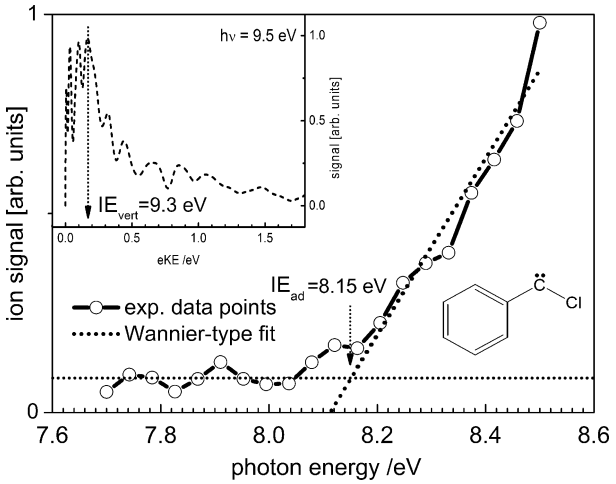

Fig. 9 From the photoionisation efficiency curve of CPC^+ an IE_{ad} = 8.15 eV can be extracted. The photoelectron spectrum, derived from the VMI photoelectron image, is given as an inset and yields IE_{vert} = 9.3 eV.

approximately and the simulation underestimates the spectral intensity at energies close to the ionisation threshold. As expected, there is significant activity in the $C_{(1)}$–$C_{(2)}$–CF_3 bend, but in addition some other low-frequency modes are active as well, including the CF_3 torsion. Due to the presence of several low-frequency modes and combination bands and the finite vibrational temperature, a resolution of the vibrational structure was not possible. Due to the large number of degrees of freedom, the poorly known vibrational temperature with pyrolysis and the absence of a suitable reference point, *i.e.* a well characterised neutral ground state, an optimisation of the experimental spectrum is difficult and the value of 8.4 eV constitutes only an approximate IE_{ad}.

A more accurate value for IE_{ad} is possibly obtained from the ion yield spectrum given in Fig. 8. At the ionisation threshold autoionising states are easily excited and contribute to the ion signal.[38] Thus an ion signal can often be observed even when the Franck–Condon factors are small and ion yield spectra provide an independent test for the accuracy of an IE determined by PES. In conventional photoelectron spectroscopy the photon energy is in general significantly higher than the ionisation energy and autoionising states close to threshold do not contribute to the signal. The ion signal in Fig. 8 was fitted by a Wannier-type threshold law,[39] indicated by the solid line. Its crossing point with the baseline, marked by an arrow, yields the adiabatic ionisation energy IE_{ad} = 8.47 eV. Signal below this value can be assigned to ionisation of vibrationally excited carbene. The IE_{ad} obtained from the ion yield spectra is in reasonable agreement with the one derived from the photoelectron spectrum, given the size of the molecule.

For CPC we recorded a photoelectron image with pyrolysis at 9.5 eV photon energy. Again only electrons arriving in coincidence with CPC^+ are considered. We derived an IE_{vert} = 9.3 eV from the photoelectron spectrum, which is given as an inset in Fig. 9, despite the inferior signal-to-noise ratio. As for TFPC the photoionisation efficiency curve was analysed to get information on the adiabatic IE, depicted in the main part of Fig. 9. From the crossing of the line obtained in the Wannier-fit with the baseline we obtain an approximate adiabatic ionisation energy of IE_{ad} = 8.15 eV. The difference between the adiabatic and the vertical ionisation energies is thus much larger for CPC than for TFPC.

Discussion

In both carbenes the $C_{(1)}$–$C_{(2)}$–X angle θ increases significantly upon ionisation. Since singlet arylcarbenes are usually bent stronger than triplet carbenes,[12] this increase is more pronounced in CPC. The difference in the angle θ can be understood within a valence shell electron pair repulsion (VSEPR) model of the carbenes[40] and is thus expected within the simple pictures of organic chemistry. The reduction of $R(C_{(1)}$–$C_{(2)})$ upon ionisation can be explained by a delocalisation of the positive charge over the aromatic ring. Thus $R(C_{(1)}$–$C_{(2)})$ gains more double bonding character. In contrast, the change in $R(C_{(1)}$–X) is opposite in the two carbenes. In CPC the non-bonding electrons on the chlorine atom can also interact with the aromatic system and the empty p-orbital on $C_{(1)}$. In the cation the chlorine donates electrons into this π-system and thus mesomerically stabilises the positive charge on $C_{(1)}$, leading to an increase in the $C_{(1)}$–Cl bond strengths and a shortening of the bond length. In contrast, a mesomeric stabilisation is not possible for the strong electron withdrawing group X = CF_3. Since fluorine is the most electronegative element, the carbon of the CF_3 group will hold a strong positive partial charge. This introduces an additional Coulomb repulsion in the cation, increasing the $C_{(1)}$–CF_3 bond length, which cannot be compensated by a hyperconjugative interaction of the C–F bond with the cationic centre. Due to the large geometry changes, Franck–Condon factors vanish around the adiabatic ionisation threshold and the difference between IE_{ad} and IE_{vert} is significant in both carbenes. This is reflected in the Franck–Condon simulations shown in Fig. 7. In agreement with the computations this difference is even more pronounced in CPC than in TFPC, rendering it even more difficult to identify the adiabatic IE. However, as shown in Table 2, the experimentally obtained IE_{ad} and IE_{vert} values differ more than the computed values. The computations also underestimate the adiabatic ionisation energies of both carbenes by more than 0.5 eV, the vertical one by almost or more than 1 eV. We thus conclude that (a) the geometry

change upon ionisation is probably even larger than computed and (b) DFT computations do not yield ionisation energies with chemical accuracy for the species under investigation. For CPC the computed numbers deviate more from the experimental data than for TFPC. It should be noted that the DFT method employed agrees quite well with experiments for neutral CPC.[8,12] This indicates that the description of the ion has to be improved for better ionisation energies. Note that the photoionisation of carbenes is unique, because both neutral and cation CPCs are open-shell systems. The IE values computed by simple DFT do not constitute a good starting point for experiments, while high-level *ab initio* methods cannot yet be applied to molecules of that size. The data thus illustrate the advantages of using a broadly tunable light source for photoionisation experiments on large carbenes. The smaller difference between IE_{ad} and IE_{vert} values found for TFPC both experimentally and computationally confirms that this carbene is indeed formed in its triplet ground state in the pyrolysis, because for singlet TFPC a change in θ very similar to CPC would be expected. Vibrational resolution was not achieved in the photoelectron spectra, because several low-frequency modes are active in both carbenes.

The different behaviour of the two diazirine precursors is also of interest. For simple diazirine, c-CH_2N_2, a photoelectron spectrum was reported in the literature[41] and numerous ionic states were identified. In contrast, CPC undergoes complete dissociative photoionisation, while for TFPC at least some molecular ions are formed at the ionisation threshold. Hybrid-DFT computations yielded a stable minimum on the ionic ground state surface for both diazirines. However, in c-CH_2N_2 the lowest ionisation energy corresponds to electron ejection from a nitrogen lone-pair which is not associated with a big change in the binding properties. In the phenyldiazirines, on the other hand, the HOMO is computed to extend over the whole molecule. As visible in Table 3 several bond lengths change upon ionisation. In the three-membered ring the C–N bonds are weakened, while the N═N binding increases. Thus the stability of the ring decreases in the ion and the thresholds for ionisation and dissociative ionisation become close. As shown in Table 3, the geometry change upon ionisation is larger for CP-diazirine. In particular a significant decrease in the $C_{(1)}$–Cl bond lengths is computed. Note that there is no experimental evidence for a stable molecular ion, although computations yielded an energy minimum, but it is possible that sufficiently large Franck–Condon factors exist only for states close to or above the threshold for dissociative ionisation. In TFP-diazirine the geometry change is not as pronounced; subsequently some molecular ions can be observed.

One can also illustrate the different behaviour of the two diazirine cations within the pictures of organic chemistry: qualitatively, the loss of N_2 will result in an sp^2 centre on $C_{(1)}$. The chlorine atom will stabilise both the product and the pathway to product formation through a mesomeric effect and thus facilitate the loss of nitrogen by lowering the barrier to dissociation. No such promotion of carbene formation is provided by the CF_3 group, which in contrast has an electron withdrawing effect. The same argument would hold for neutral diazirines. In fact, neutral TFP-diazirine is stable and used for photolabelling (*vide supra*), while CP-diazirine is explosive.

In principle, binding energies of neutral molecules can be derived from ionisation and appearance energies through thermochemical cycles, provided that dissociation in the ion proceeds barrierless. From the AE (TFP-N_2^+, $TFPC^+$) and the IE of TFPC one could derive a binding energy for neutral TFP-N_2. However, the decomposition of the neutral diazirines is generally known to be strongly exothermic. In addition, our computations indicate the existence of a reverse barrier for the reaction $TFPC^+ + N_2$. Any value for the binding energy of the neutral thus has to be considered unreliable. From the IE of the TFP-N_2 we calculate an energy barrier of 0.3 eV for the dissociation of TFP-N_2^+.

Summary

The photoionisation of two phenylcarbenes, chlorophenylcarbene and trifluoromethylphenylcarbene has been explored using tunable synchrotron radiation in the VUV range. Carbenes have been generated cleanly by jet flash pyrolysis in a continuous beam, as demonstrated by time-of-flight mass spectra and ion images. Due to the large geometry change upon ionisation the photoelectron spectra, derived from velocity-mapped photoelectron images, are broad and unstructured and show no vibrational resolution. Adiabatic ionisation energies have been extracted from ion yield spectra, $IE_{ad}(CPC) = 8.15$ eV and $IE_{ad}(TFPC) = 8.47$ eV. For TFPC it is in reasonable agreement with the value obtained from a Franck–Condon simulation of the photoelectron spectrum (8.4 eV), but we believe that the IE_{ad} from ion yield spectra is more accurate. The vertical ionisation energies lie at $IE_{vert}(CPC) = 9.30$ eV and $IE_{vert}(TFPC) = 8.95$ eV. In computations on CPC one finds not only a large increase in the angle θ, but also a significant reduction in the C–Cl bond length, indicating that the non-bonding electrons of the chlorine atom interact with the π-system of the cation of the carbene. In TFPC the geometry change is also pronounced, but not as large. The adiabatic and vertical ionisation energies are underestimated by more than 0.5 eV in the calculations, showing the advantages of a broadly tunable light source for photoionisation studies of carbenes.

In addition, the diazirine precursors were investigated. It was found that chlorophenyldiazirine undergoes complete dissociative photoionisation to CPC^+ and N_2. This process starts at around 8.80 eV. In experiments on trifluoromethylphenyldiazirine some molecular ions were detected above 9.05 eV. However, dissociative ionisation to $TFPC^+ + N_2$ also sets in right at this energy. From a fit to the data an appearance energy of 9.27 eV was derived for the dissociative photoionisation of TFP-diazirine.

Acknowledgements

This work was financially supported by the Deutsche Forschungsgemeinschaft. B.N. acknowledges a fellowship by the Fonds der Chemischen Industrie. Travel subsidies were provided by SOLEIL through the European Commission programme "Transnational access to research infrastructures" and by the German–French binational PROCOPE program. We would like to thank the staff at SOLEIL for operating the

storage ring and for technical support on the DESIRS beamline, in particular Jean-François Gil, Nelson De Oliveira and Laurent Nahon. We also thank Séverine Boyé-Péronne, Stéphane Douin and Bérenger Gans for their contributions to the experiment.

References

1 P. Chen, in *Advances in Carbene Chemistry*, ed. U. H. Brinker, JAI, New York, 1998.
2 I. Fischer, *Int. J. Mass Spectrom.*, 2002, **216**, 131.
3 K.-C. Lau and C. Y. Ng, *J. Chem. Phys.*, 2005, **122**, 224310.
4 T. Schüßler, H.-J. Deyerl, S. Dümmler, I. Fischer, C. Alcaraz and M. Elhanine, *J. Chem. Phys.*, 2003, **118**, 9077.
5 T. Schüßler, W. Roth, T. Gerber, I. Fischer and C. Alcaraz, *Phys. Chem. Chem. Phys.*, 2005, **7**, 819.
6 I. Fischer, T. Schüßler, H.-J. Deyerl, M. Elhanine and C. Alcaraz, *Int. J. Mass Spectrom.*, 2007, **261**, 227.
7 H. F. Bettinger, P. R. Schreiner, P. v. R. Schleyer and H. F. Schaefer III, in *Encyclopedia of Computational Chemistry*, ed. P. v. R. Schleyer, Wiley, Chichester, 1998.
8 B. Noller, L. Poisson, R. Maksimenka, I. Fischer and J.-M. Mestdagh, *J. Am. Chem. Soc.*, 2008, **130**, 14908.
9 I. R. Gould, N. J. Turro, J. Butcher Jr., C. Doubleday Jr., N. P. Hacker, G. F. Lehr, R. A. Moss, D. P. Cox, W. Guo, R. C. Munjal, L. A. Perez and M. Fedorynski, *Tetrahedron*, 1985, **41**, 1587.
10 M. G. Rosenberg and U. H. Brinker, *J. Org. Chem.*, 2003, **68**, 4819.
11 G. A. Ganzer, R. S. Sheridan and M. T. H. Liu, *J. Am. Chem. Soc.*, 1986, **108**, 1517.
12 J. R. Pliego Jr., W. B. de Almeida, S. Celebi, Z. Zhu and M. S. Platz, *J. Phys. Chem. A*, 1999, **103**, 7481.
13 E. Wasserman, *J. Chem. Phys.*, 1965, **42**, 3739.
14 B. Noller, L. Poisson, R. Maksimenka, O. Gobert, I. Fischer and J.-M. Mestdagh, *J. Phys. Chem. A*, 2009, **113**, 3041.
15 A. Blencowe and W. Hayes, *Soft Matter*, 2005, **1**, 178.
16 L. Nahon, C. Alcaraz, J. L. Marlats, B. Lagarde, F. Polack, R. Thissen, D. Lepere and K. Ito, *Rev. Sci. Instrum.*, 2001, **72**, 1320.
17 O. Marcuille, P. Brunelle, O. Chubar, F. Marteau, M. Massal, L. Nahon, K. Tavakoli, J. Veteran and J.-M. Filhol, *AIP Conf. Proc.*, 2007, **879**, 311.
18 B. Mercier, M. Compin, C. Prevost, G. Bellec, R. Thissen, O. Dutuit and L. Nahon, *J. Vac. Sci. Technol., A*, 2000, **18**, 2533.
19 M. Richard-Viard, A. Delboulbe and M. Vervloet, *Chem. Phys.*, 1996, **209**, 159.
20 T. Baer and P.-M. Guyon, in *High Resolution Laser Photoionisation and Photoelectron Studies*, ed. C. Y. Ng, T. Baer and I. Powis, Wiley, New York, 1995.
21 T. Baer, *Int. J. Mass Spectrom.*, 2000, **200**, 443.
22 G. A. Garcia, L. Nahon, C. J. Harding, E. A. Mikajlo and I. Powis, *Rev. Sci. Instrum.*, 2005, **76**, 053302.
23 G. A. Garcia, H. Soldi-Lose and L. Nahon, *Rev. Sci. Instrum.*, 2009, **80**, 023102.
24 D. Céolin, G. Chaplier, M. Lemonnier, G. A. Garcia, C. Miron, L. Nahon, M. Simon, N. Leclercq and P. Morin, *Rev. Sci. Instrum.*, 2005, **76**, 043302.
25 G. A. Garcia, L. Nahon and I. Powis, *Rev. Sci. Instrum.*, 2004, **75**, 4989.
26 D. W. Kohn, H. Clauberg and P. Chen, *Rev. Sci. Instrum.*, 1992, **63**, 4003.
27 R. A. Moss, *Acc. Chem. Res.*, 2006, **39**, 267.
28 W. H. Graham, *J. Am. Chem. Soc.*, 1965, **87**, 4396.
29 J. Brunner and F. M. Richards, *J. Biol. Chem.*, 1980, **255**, 3319.
30 G. K. Jarvis, K. M. Weitzel, M. Malow, T. Baer, Y. Song and C. Y. Ng, *Phys. Chem. Chem. Phys.*, 1999, **1**, 5259.
31 K. M. Weitzel, M. Malow, G. K. Jarvis, T. Baer, Y. Song and C. Y. Ng, *J. Chem. Phys.*, 1999, **111**, 8267.
32 T. Baer, B. Sztaray, J. P. Kercher, A. F. Lago, A. Bödi, C. Skull and D. Palathinkal, *Phys. Chem. Chem. Phys.*, 2005, **7**, 1507.
33 C. Lee, W. Yang and R. G. Parr, *Phys. Rev. B: Condens. Matter*, 1988, **37**, 785.
34 M. J. Frisch, G. W. Trucks, H. B. Schlegel, G. E. Scuseria, M. A. Robb, J. R. Cheeseman, J. A. Montgomery, Jr., T. Vreven, K. N. Kudin, J. C. Burant, J. M. Millam, S. S. Iyengar, J. Tomasi, V. Barone, B. Mennucci, M. Cossi, G. Scalmani, N. Rega, G. A. Petersson, H. Nakatsuji, M. Hada, M. Ehara, K. Toyota, R. Fukuda, J. Hasegawa, M. Ishida, T. Nakajima, Y. Honda, O. Kitao, H. Nakai, M. Klene, X. Li, J. E. Knox, H. P. Hratchian, J. B. Cross, V. Bakken, C. Adamo, J. Jaramillo, R. Gomperts, R. E. Stratmann, O. Yazyev, A. J. Austin, R. Cammi, C. Pomelli, J. Ochterski, P. Y. Ayala, K. Morokuma, G. A. Voth, P. Salvador, J. J. Dannenberg, V. G. Zakrzewski, S. Dapprich, A. D. Daniels, M. C. Strain, O. Farkas, D. K. Malick, A. D. Rabuck, K. Raghavachari, J. B. Foresman, J. V. Ortiz, Q. Cui, A. G. Baboul, S. Clifford, J. Cioslowski, B. B. Stefanov, G. Liu, A. Liashenko, P. Piskorz, I. Komaromi, R. L. Martin, D. J. Fox, T. Keith, M. A. Al-Laham, C. Y. Peng, A. Nanayakkara, M. Challacombe, P. M. W. Gill, B. G. Johnson, W. Chen, M. W. Wong, C. Gonzalez and J. A. Pople, *GAUSSIAN 03 (Revision B.04)*, Gaussian, Inc., Wallingford, CT, 2004.
35 P. Csaszar and P. Pulay, *J. Mol. Struct.*, 1984, **114**, 31.
36 Details of the computations are available from the authors upon request.
37 P. Imhof, D. Krügler, R. Brause and K. Kleinermanns, *J. Chem. Phys.*, 2004, **121**, 2598.
38 J. Berkowitz, *Photoabsorption, Photoionization and Photoelectron Spectroscopy*, Academic Press, New York, 1979.
39 G. H. Wannier, *Phys. Rev.*, 1953, **90**, 817.
40 R. J. Gillespie and I. Hargittai, *The VSEPR Model of Molecular Geometry*, Allyn & Bacon, Englewood Cliffs, NJ, 1991.
41 M. B. Robin, C. R. Brundle, N. A. Kuebler, G. B. Ellison and K. B. Wiberg, *J. Chem. Phys.*, 1972, **57**, 1758.